Chapter 2
Synthesis of Ti-MWW Zeolite

Abstract Titanosilicate with MWW topology can be prepared by hydrothermal method, dry-gel method, and post-synthesis method. At first, the addition of B atoms in the synthesis gels was identified as the key factor for the successful synthesis of Ti-MWW under hydrothermal condition. Then, several alternative methods, for example, hydrothermal method with dual SDAs and post-synthesis method, were developed to provide B-less or B-free condition, which avoided a waste of B atoms as well as the framework acidity introduced by B atoms. Ti-MWW zeolites prepared by different methods varied in particle size and activity in liquid oxidation reactions, for example, the epoxidation of 1-hexene.

Keywords Ti-MWW · Synthesis · B content · Post-synthesis method · Epoxidation

2.1 Introduction

The first titanosilicate TS-1 has achieved great success in the area of redox catalysis [1, 2]. It is not only highly efficient but also zero waste disposal, several zeolite structures with larger pores have been chosen as candidates for synthesizing titanosilicates such as MOR [3], BEA [4], MTW [5]. The purpose is to overcome the deficiencies that the medium-pore TS-1 catalyst meets with less activity in the oxidation involving the substrates with large molecular dimensions. Post-synthesized Ti-MOR with one-dimension 12-MR channels has been proved to be highly active in the ammoximation of ketones [6] and the hydroxylation of dutrex [7]. However, Ti-MOR is almost inactive in the epoxidation of alkenes. Although Ti-MOR zeolite possesses larger-pore channels than TS-1, their channels are not inter-connective [8]. This makes it lack the potential activity possessed by the zeolites with three-dimensionally (3D) connected channels. Ti-Beta with a 3D

P. Wu et al., *MWW-Type Titanosilicate*,
SpringerBriefs in Green Chemistry for Sustainability,
DOI: 10.1007/978-3-642-39115-6_2, © The Author(s) 2013

12-MR pore system shows advantages in the epoxidation of cyclic alkenes with H_2O_2, but it is intrinsically less active than TS-1 in the reactions involving the small-size substrates, which is due to the large amount of defects in the Beta structure [9]. Moreover, the leaching of Ti species during the liquid phase reactions is very obvious for Ti-Beta zeolite. Apart from microporous zeolites, Ti-containing mesoporous zeolites such as Ti-MCM-41[10] have also been prepared and they showed high activity only when *tert*-butyl hydroperoxide (TBHP) was adopted as the oxidant. The low mechanical and hydrothermal stability, easy leaching of Ti species in liquid phase reactions, and lower intrinsic activity make Ti-MCM-41 less active than TS-1 when the substrates do not suffer diffusion hindrance problems.

MWW-type zeolite, with two independent set of 10-MR channels, was first constructed from a lamellar precursor by calcination, during which dehydration and condensation take place to form 3D MWW structure [11]. Those diffraction peaks related to the layer stacking direction, *c*-direction, would disappear upon calcination while other diffraction peaks due to the MWW sheets are almost intact. Aluminum containing MWW-type zeolite, well known as MCM-22, has shown great success in the process of benzene alkylation as a solid acid catalyst since it was found, mainly owing to its unique structure [12]. In addition to two independent sets of 10-MR channels, the MWW structure possesses also 12-MR supercages ($0.7 \times 0.7 \times 1.8$ nm), which turn to be pockets or cup moieties (0.7×0.7 nm) on the crystal outer surface. The intracrystalline supercages and exterior pockets covering the hexagonal flake-like crystals are considered to serve as the open reaction spaces for the disproportionation of toluene and alkylation of benzene. Considering that the MWW-type structure is stable and unique, it is supposed to show unusual activity as a redox catalyst when the transition metal cations are incorporated into the framework. Unfortunately, the road for preparing Ti containing MWW-type (Ti-MWW) zeolite was not as smooth as that of trivalent cations containing MWW zeolites such as Al-MWW [13], B-MWW [14] and Fe-MWW [15].

Ti-containing zeolites are prepared mainly by direct hydrothermal method [16], post-synthesis method [17], and dry-gel conversion (DGC) method [18]. Different from the aluminosilicates, the synthetic system for preparing titanosilicates with high activity should contain as small amount of other metal ions as possible, which means a high siliceous synthetic gel is preferred for preparing Ti-containing zeolites. However, some zeolite structures such as MOR zeolite cannot be constructed in siliceous gels if without the help of Al^{3+} and Na^+ cations [19]. Post-synthesis method was then employed as another effective way to prepare those titanosilicates which cannot be directly synthesized by the hydrothermal method. In this sense, Ti-MOR was successfully post-synthesized using a so-called “atom-planting” route, which involved the gas–solid reaction between highly dealuminated MOR zeolite and $TiCl_4$ vapor at elevated temperatures [6]. Grafting technique is also a useful post-synthesis method especially in preparing Ti-containing Mesoporous materials such as Ti-MCM-41[20] and Ti-SBA-15 [21]. The DGC method involves the dehydration of synthetic gels and the

crystallization assisted by steam that is placed separately from the synthetic gel powder. The DGC method has achieved a great success in preparing Ti-Beta with less Al^{3+} content and smaller crystal size than conventional hydrothermal synthesis [22].

Hydrothermal synthesis is the most widely used method to prepare zeolites including both pure silicate zeolites and metal-doped zeolites. However, it is difficult to obtain Ti-MWW from the synthetic gels only containing silicon and titanium via hydrothermal method. Since the direct synthesis of Ti-MWW was not so easy, the post-synthesis method became an alternative. The first success of the titanosilicate with the MWW topology is Ti-ITQ-2 [23], which was prepared by grafting titanocene onto the surface of delaminated ITQ-2 silicalite. ITQ-2, containing abundant silanols exposed on the surface, is a delaminated form of the MWW structure. Nevertheless, Ti-ITQ-2 zeolite shows high activity only when using TBHP as an oxidant, showing very similar catalytic behaviors to mesoporous titanosilicates such as Ti-MCM-41. It is the hydrophilic character that leads to a low activity of Ti-ITQ-2 in H_2O_2 system and Ti leaching during liquid-phase reactions. Atom-planting technique is another post-synthesis method adopted to prepare Ti-MWW zeolite, in which gas phase $TiCl_4$ was used as Ti source to react with dealuminated Al-MCM-22 zeolite [24]. However, severe leaching of Ti species occurs in the Ti-MWW zeolite obtained by atom-planting method. Although there are so many difficulties in the synthesis of Ti-MWW zeolite, the above efforts are not in vain but pave the way for the following study.

The breakthrough in the synthesis of Ti-MWW zeolite with both high crystallinity and activity was the introduction of boric acid as structure-supporting agent, which was based on the synthesis of B-containing MWW zeolite ERB-1 [25]. ERB-1 zeolite can be synthesized both in the presence and the absence of alkali cations, which means B^{3+} cations can serve as structure-supporting agent. Borosilicate with the MWW topology can be obtained from the gels with Si/B = 1.5. However, Ti-MWW zeolite cannot be synthesized in the gels with Si/B = 1.5 unless a large amount of boron cations were introduced with Si/B = 0.75 [26]. Although the acidity of B^{3+} ions is much weaker than that of Al^{3+} ions, the introduction of B atom into the MWW framework would inevitably increase the electronegativity and further affect the performance of the Ti species in catalysis. Hence, several other methods (Table 2.1) such as F^- ions assisted method, DGC method [27] and post-synthesis method [28] were also employed to prepare Ti-MWW zeolite with the aim of decreasing the B content. Ti-MWW zeolites prepared with different methods varied in particle sizes and activity. These methods can be divided into three kinds based on the B content in synthetic gels: B-containing method, B-less method, and B-free method. All the synthesis methods are explained in detail in following text.

Table 2.1 A summary of synthesis methods for Ti-MWW[a]

No.	Si source	SDA[b]	Method[c]	Gel composition		Crystal size (μm)[d]		Ref.
				Si/B	Si/Ti			
1	TEOS	PI, HMI	HTS	0.75	10 ~ ∞	PI	(0.2–0.5)* (0.05–0.1)	[26]
						HMI	1*0.1	
2	Fumed silica	OCTMAOH HEPMAOH HEXMAOH	HTS	5–10	30 ~ ∞	0.15*0.02		[41]
3	Fumed silica	TMAadOH and HMI	HTS	∞	20 ~ ∞	0.5*0.1		[57]
4	Fumed silica Colloidal silica	PI, HMI	DGC	1–92	30 ~ ∞	4–8		[27]
5	TEOS Fumed silica	PI, HMI	F^-	1–15	15 ~ ∞	2*0.2		–
6	Siliceous MWW	PI, HMI	PS	∞	20 ~ ∞	PI	(0.2–0.5)* (0.05–0.1)	[28]
						HMI	1*0.1	

[a] The Ti source used in all the syntheses is tetrabutylorthotitanate (TBOT)
[b] *PI* piperidine, *HMI* hexamethyleneimine, *OCTMAOH* octyltrimethylammonium hydroxide, *HEPMAOH* heptyltrimethylammonium hydroxide, *HEXMAOH* hextyltrimethylammonium hydroxide, *TMAadOH N,N,N*-trimethyl-1-adamantanammonium hydroxide
[c] *HTS* hydrothermal synthesis, *DGC* dry gel conversion; *F^-* crystalized with the assistant of F^- ions, *PS* postsynthesis
[d] Crystal size is presented as the length multiplied by the thickness

2.2 Boron-Containing Ti-MWW Synthesis

With the assistance of boric acid, Ti-MWW zeolite (denoted as Ti-MWW-HTS) was hydrothermally synthesized for the first time in a series of Ti-content with the Si/Ti ratios ranging from 10 to ∞. It can be seen from Table 2.2 that only a small portion of the B^{3+} cations in the synthetic gels was incorporated into the framework of Ti-MWW zeolite, which means that most of the B^{3+} cations were useless in constructing the MWW structure [26]. The case was exactly the contrary as for Ti^{4+} cations. Ti^{4+} cations added in the synthetic gels were all incorporated into the Ti-MWW-HTS zeolite, although the crystallinity was slightly decreased with the increase of Ti content. The insertion of Ti^{4+} into the framework has been proved by both UV–Vis and IR measurements.

Two adsorption bands were observed in the UV–visible spectra (Fig. 2.1), locating around 220 and 260 nm, respectively, which indicate there are two kinds of Ti species in the as-synthesized Ti-MWW zeolite. The band around 220 nm is due to the tetrahedral Ti species [29] in the framework of Ti-MWW-HTS zeolite while the band around 260 nm is attributed to the octahedral Ti species [30] on the external surface of the zeolite. Irrespective of a high Ti content like Si/Ti ratio of 20 in the gel, anatase phase was never detected, indicating the Ti species were highly dispersed. The presence of 260 nm adsorption-related octahedral species is

Table 2.2 Hydrothermal synthesis of Ti-MWW from different gel compositions

No.	Gel composition[a]		Product composition and surface area					
	Si/B	Si/Ti	Ti-MWW-PI			Ti-MWW-HMI		
			Si/B	Si/Ti	SSA[b] (m^2 g^{-1})	Si/B	Si/Ti	SSA[b] (m^2 g^{-1})
1	0.75	∞	11.8	∞	616	13.6	∞	601
2	0.75	100	12.6	120	625	16.3	138	621
3	0.75	70	12.2	63	612	14.2	79	628
4	0.75	50	11.4	51	621	12.4	53	–
5	0.75	30	11.0	31	623	11.6	31	613
6	0.75	20	12.7	21	540	11.4	22	–[c]
7	0.75	10	13.6	10	537	11.5	9.6	541

Reprinted from Ref. [26], Copyright 2001, with permission from American Chemical Society
[a] Other gel compositions: PI or HM/SiO_2 = 1.4; H_2O/SiO_2 = 19
[b] *SSA* specific surface area (Langmuir)
[c] Not determined

simply because as-synthesized Ti-MWW-HTS has a lamellar precursor structure. Those Ti species introduced on the layer surface tend to occupy the octahedral coordination. This is an unusual aspect greatly different from those titanosilicates which have the 3D crystalline structures already in as-synthesized form.

Both piperidine (PI) and hexamethyleneimine (HMI) serve as the structure-directing agents (SDA) in preparing Ti-MWW-HTS zeolite, denoted as Ti-MWW-HTS-PI and Ti-MWW-HTS-HMI, respectively. They possess almost the same surface area (Table 2.2), but the particle size of Ti-MWW-HTS-HMI is larger than Ti-MWW-HTS-PI, which induces the difference of Ti^{4+} distribution on the crystal of Ti-MWW zeolite. As a result, Ti-MWW-HTS-PI with smaller particle size and larger external surface area possesses more Ti species on the external surface than Ti-MWW-HTS-HMI, which induces a main adsorption band around 260 nm in UV–Vis spectra. As for Ti-MWW-HTS-HMI, the main adsorption band changes from 220 to 260 nm with the increase of Ti content, which means Ti^{4+} ions take place the intracrystalline position in priority. When the as-synthesized Ti-MWW-HTS zeolites were suffered with calcination treatment, a new band around 330 nm appeared on both the UV–visible spectra of Ti-MWW-HTS-PI and Ti-MWW-HTS-HMI, indicating an anatase phase [31] formed probably due to the partial condensation and aggregation of neighboring surface Ti species upon calcination. These extraframework Ti species should be removed because it would cause the unproductive decomposition of hydrogen peroxide in actual reactions, which would certainly lead to a poor performance of Ti-MWW zeolite as an oxidation catalyst. An acid treatment was employed to remove the inactive Ti species in the calcined form of Ti-MWW-HTS zeolite. As indicated by the UV–visible spectra, the acid treatment decreased slightly the bands around 220 and 260 nm, while it hardly affected the band around 330 nm. This revealed that the anatase phase can withstand the acid treatment and hardly be removed from the Ti-MWW-HTS zeolite once the anatase phase formed during calcination.

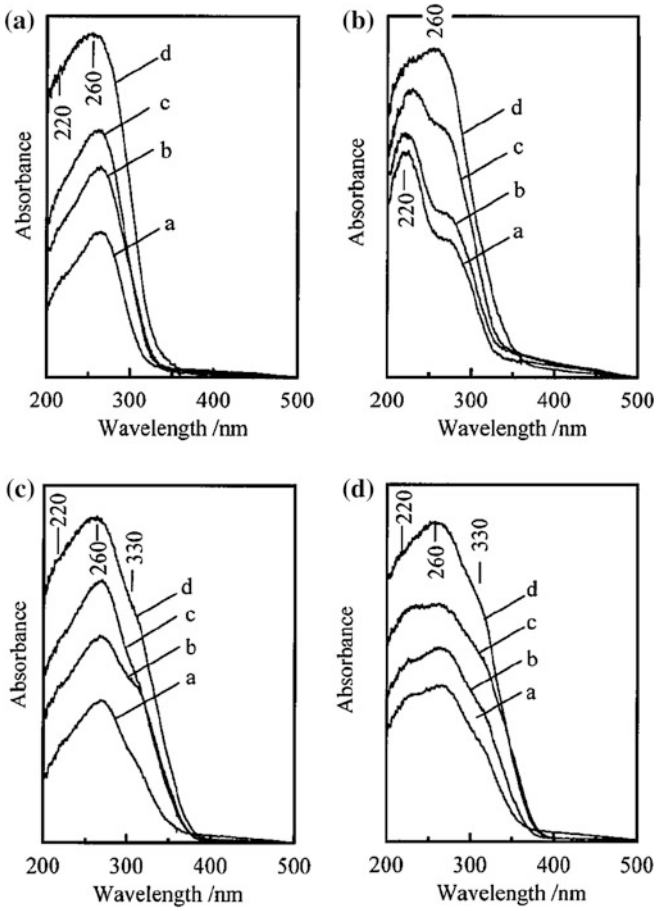

Fig. 2.1 UV–visible spectra of (**a**) as synthesized and (**c**) calcined Ti-MWW-PI, and (**b**) as-synthesized and (**d**) calcined Ti-MWW-HMI with the Si/Ti ratio of (*a*) 100, (*b*) 50, (*c*) 30, (*d*) 10. Reprinted from Ref. [26], Copyright 2001, with permission from American Chemical Society

Then the acid extraction was tried on the as-synthesized Ti-MWW-HTS zeolite with the purpose of removing the anatase phase from the precursor in advance of the calcination treatment. The XRD pattern of the acid treated Ti-MWW-HTS zeolite was almost the same as that of calcined Ti-MWW-HTS zeolite, with 001 and 002 diffractions disappeared, which was probably due to the removal of support such as Ti and organic molecules between the layers. UV–visible spectra verified that the octahedral Ti species on the external surface of Ti-MWW crystals were removed selectively upon the acid treatment. Further calcination made the diffraction peaks more intense and resulted in an anatase-free Ti-MWW-HTS zeolite as verified by the UV–visible spectra again. It should be pointed out that the octahedral Ti species cannot be fully removed by acid treatment in the case of

Ti-MWW-HTS lamellar precursors with Si/Ti ratio lower than 20. Nevertheless, the tetrahedral Ti species were almost intact in the framework during acid treatment procedure. In such an acid and subsequent calcination procedure, the inactive Ti species were almost removed and the B content was also decreased a lot. If a further acid treatment was adopted, a nearly B-free Ti-MWW zeolite was obtained while the Ti content was almost unchanged during the second round of acid treatment. As shown in Fig. 2.2, Ti-MWW nearly free of both B and anatase can be synthesized with PI or HMI as SDA under alkali-free conditions, followed by a

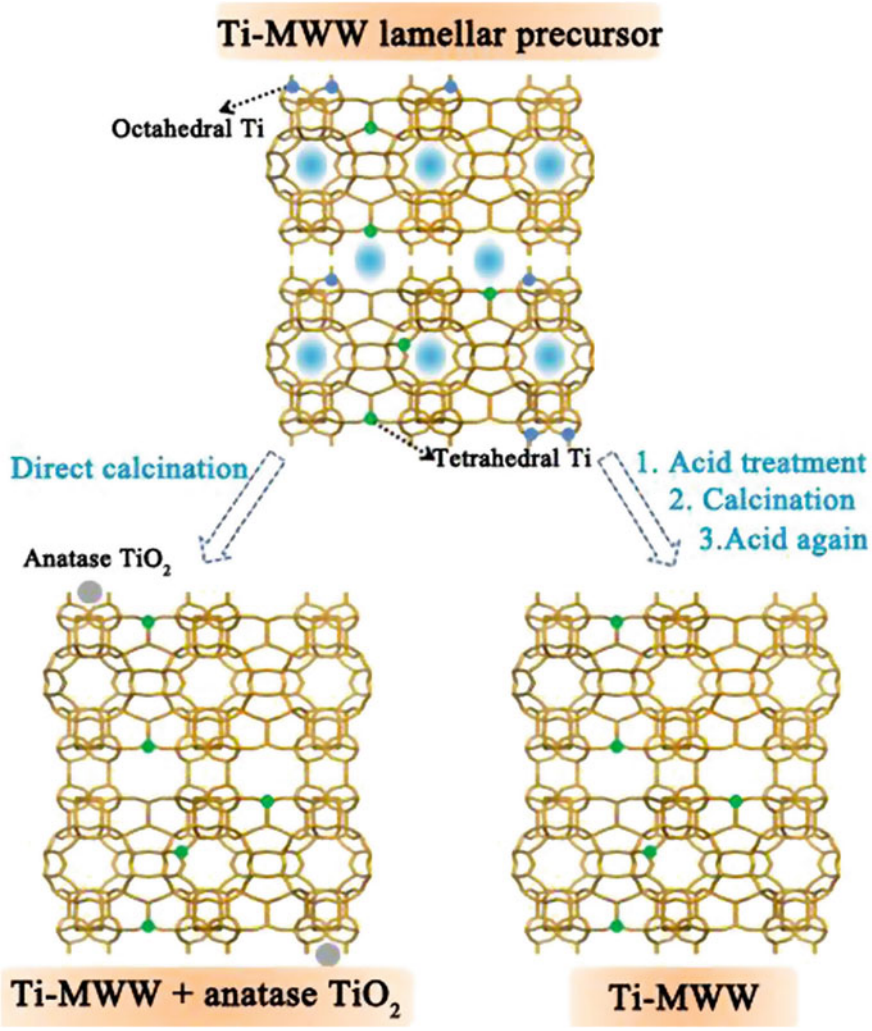

Fig. 2.2 MWW-type titanosilicate containing only tetrahedral Ti species in the framework was prepared by a cyclic acid treatment

cyclic post-treatment, that is, an acid treatment, subsequent calcination and a further acid treatment.

A detailed study on the performance of Ti-MWW-HTS zeolite in the epoxidation of alkenes revealed that Ti-MWW-HTS showed a superior activity independent of the oxidant in comparison with microporous TS-1 and Ti-MOR and mesoporous Ti-MCM-41 [32]. As compared with Ti-Beta zeolite, Ti-MWW showed a better performance in the epoxidation of cyclohexene using TBHP as the oxidant. However, Ti-Beta zeolite showed a higher activity in the case of H_2O_2 as the oxidant. The stabilities of both structure and active species are most concerned factors in judging a catalyst. The Ti content was almost unchanged in the liquid-phase cyclohexene epoxidation, while the B content decreased nearly half of the fresh catalyst after the first use and further decreased gradually with the reaction–regeneration cycles (Fig. 2.3a). B atoms much smaller than silicon atoms are easily cleaved from the framework, forming defects simultaneously. Two kinds of regeneration treatment were applied including washing with acetone and calcination (Fig. 2.3b). The activity was recovered only 75 % upon washing with acetone while the turnover number (TON) was totally restored by calcination. The severe leaching of B atoms would leave vacancy and then cause the Ti migration upon the rearrangement of the framework occurring in the vicinity of B cations. The regeneration treatment of calcination was supposed to mend those defects and then to stabilize the framework as well as the Ti species.

As mentioned above, B atoms involved in the framework was expected to have weaker influence on the catalytic behaviors of the Ti sites than the Al atoms. A detailed study of B effect was investigated in the epoxidation of cyclohexene, which revealed that the B content exhibited almost no influence on the conversion

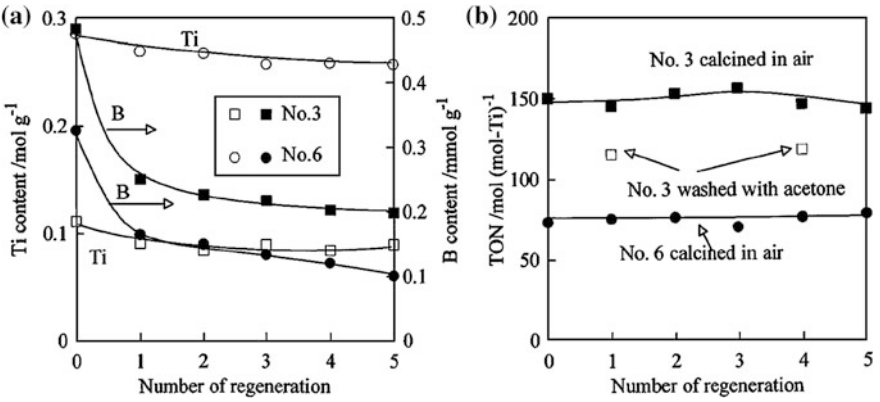

Fig. 2.3 Changes of the Ti and B contents (**a**) and that of the TON for the cyclohexene conversion (**b**) with the cycle of reaction–regeneration. Cyclohexene oxidation: 0.05 g Ti-MWW, 10 mmol of substrate, 5 mmol of H_2O_2, 5 mL of acetonitrile; temp., 333 K; time, 2 h. *No. 3* indicates Ti-MWW-PI(100) treated by 2 M HNO_3, while *No. 6* indicates Ti-MWW-PI(70) treated by 6 M HNO_3. Reprinted from Ref. [32], Copyright 2001, with permission from Elsevier

of cyclohexene but increased the selectivity to ring-opening products. The existence of B atoms in the framework of Ti-MWW zeolite would not poison the Ti active sites but arouse the ring-opening and solvolysis reactions of the target epoxide product due to the weak acidity related to the Si(OH)B groups.

The conversion of 1-hexene increased with the increase of Ti content, while the TON value showed a volcanic shape change (Fig. 2.4). On the contrary, the TON value decreased with the increase of Ti content when the epoxidation of cyclohexene was carried out over Ti-MWW zeolite. The two different variations were believed to be related to the molecular size and the distribution of Ti species in the Ti-MWW crystals. Ti species can be located in three kinds of sites in the Ti-MWW zeolite, that is, the 10-MR channels, the intracrystalline supercages, and the external surface 12-MR pockets. 1-Hexene molecules were small enough to diffuse into the 10-MR channels and access all the Ti species, whereas the cyclohexene molecules can only reach the supercages and the outer surface pockets. With the increase of Ti content, the Ti atoms would occupy the intracrystalline positions in priority then the outer surface, which has been proved by the UV–visible spectra [26]. When the Si/Ti ratio was higher than 40, the Ti species were almost located in the inner space of the Ti-MWW crystalline, where the larger molecules are less easily to access to. As a result, the TON values were decreased as for cyclohexene and increased as for 1-hexene with the increase of Ti content. However, when the octahedral Ti species appeared with an extreme excess amount, it is impossible to remove them completely by acid treatment, certainly causing a decrease of the TON values in both cyclohexene and 1-hexene epoxidation when the Si/Ti ratio was lower than 40.

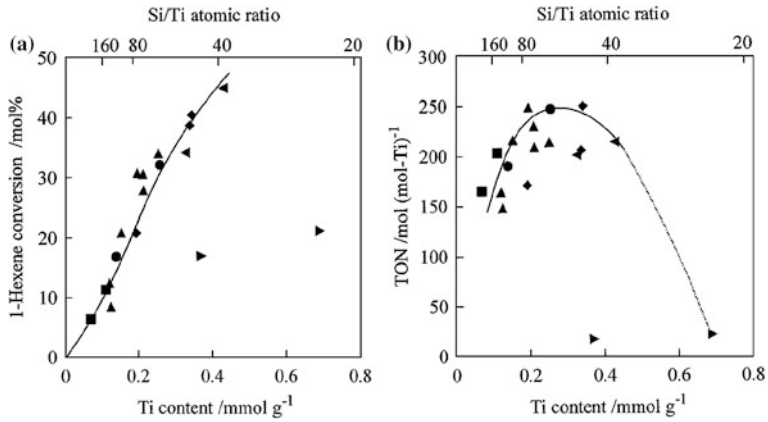

Fig. 2.4 Dependence of the conversion (**a**) and the TON (**b**) on the Ti content for the oxidation of 1-hexene with H_2O_2. Ti–MWW–PI catalysts used were prepared from the lamellar precursors with a Si/Ti ratio of 100 (*filled square*), 70 (*filled circle*), 50 (*filled up-pointing triangle*), 30 (*filled diamond*), 20 (*filled left-pointing triangle*), and 10 (*filled right-pointing triangle*). Reprinted from Ref. [32], Copyright 2001, with permission from Elsevier

2.3 Boron-Less Ti-MWW Synthesis

2.3.1 Synthesis of Ti-MWW Using Linear-Type Quaternary Alkylammonium Hydroxides

Organic SDAs play important roles in the nucleation and crystallization process of the zeolite synthesis, including compensating the structural electronegativity, filling the pore channels to stabilize the whole zeolite structure and interacting with the inorganic species to direct the formation of zeolite structures [33, 34]. All the MWW analogues are commonly synthesized with cyclic or polycyclic amine [26]. HMI was used to synthesize PHS-3 [35] and MCM-22 [26] zeolites under alkali conditions, while a special organic cations *N*,*N*,*N*-trimethyl-1-adamantylammonium ($TMAda^+$) was employed to construct SSZ-25 [36, 37] with the help of K^+ cations. These organic molecules with large molecular sizes seem to prefer to occupy the interlayer space rather than stabilize the zeolite structure. On the other hand, linear-type organic ammonium molecules have also been used to prepare zeolite with MWW topology, such as *N*,*N*,*N*,*N*′,*N*′,*N*′-hexamethyl-1,5-pentanediammonium and 1,4-*bis*(*N*-methylpyrrodinium)butane, although their structure-directing ability is relatively weak [38, 39]. The linear-type organic additives with relatively smaller sizes are more flexible than cyclic molecules and may fill both the interlayer space and the intralayer 10-MR channels in MWW structure. Liu et al. found that a linear quaternary ammonium, octyltrimethylammonium hydroxide (OCTMAOH), had the ability to direct borosilicate and titanosilicate with MWW topology under alkali-free conditions [40]. MWW borosilicate with a high crystallinity was obtained at OCTMAOH/Si ratio of 0.3, which was much smaller than the ratio required for HMI or PI. The appropriate Si/B ratio for a pure MWW borosilicate was proved to range from 10 to 20, while a structure similar to MCM-56 would emerge when the Si/B ratio was out of that range. However, a higher B content would favor the synthesis of MWW titanosilicate [41], since the introduction of Ti atoms severely hinder the crystallization process. More Ti atoms can be introduced into the MWW zeolite when the B content was maintained at a relatively high level, i.e., with a Si/B ratio of 5. The particle size of Ti-MWW zeolite synthesized using OCTMAOH as SDA was smaller than those prepared with PI and HMI molecules, which was supposed to favor the diffusion of substrate molecules and to improve the catalytic activity. Similar to above-mentioned synthesis with PI and HMI, there was a broad band in the UV–Vis spectrum of the Ti-MWW zeolite as-synthesized with OCTMAOH, indicating tetrahedral and octahedral Ti species co-existed in the obtained Ti-MWW lamellar precursor. An acid treatment and subsequent calcination can remove the octahedral and anatase Ti species selectively, with the active tetrahedral Ti species remaining in the framework of MWW. Unlike the Ti-MWW zeolite prepared with HMI or PI, more than half of the Ti atoms were removed during the post-treatment procedures. That is probably because the Ti species involved in the part of Ti-MWW zeolite with a relatively poor crystallinity can be

removed easily, which again suggested that the introduction of Ti atoms largely decrease the crystallinity. With a smaller particle size, Ti-MWW prepared with OCTMAOH showed comparable activity with those prepared with PI or HMI, mainly again due to a poor crystallinity.

The effect of alkali cations as well as another two linear-type ammoniums was also investigated following the above study. As shown in Table 2.3, OCTMAOH has stronger directing ability than both heptyltrimethylammonium hydroxide (HEPMAOH) and hextytrimethylammounium hydroxide (HEXAMOH), and the addition of alkali cations was helpful to the crystallization process when it was maintained at an appropriate ratio of K/Si = 0.04–0.06. Both the chemical element analysis (Table 2.4) and ^{13}CNMR analysis (Fig. 2.5) verified that the SDA molecules all well maintained their chemical structures during the crystallization process. Broadness and overlap of the resonance were observed in the ^{13}C NMR spectra of Ti-MWW zeolites compared with that of free SDA dissolved in dimethyl sulfoxide (DMSO), which was presumed to be related to the geometric constrain and van der Waals interactions with the zeolite frameworks. In the TG analysis, there were two kinds of weight loss, that is, below 473 K region and above 473 K region. The former weight loss was due to physical adsorbed water molecules while the latter was supposed to be caused by the decomposition of the organic SDAs. After an acid treatment, the weight loss above 473 K was decreased by about 50 wt% (Table 2.4), which indicated that about half of the SDAs were located in the interlayer space while the other half were remaining stuck in the intralayer 10-MR channels. These linear-type SDAs can diffuse into different channels without any constrains, not only filling the pores but also stabilizing the whole structure. Acid and subsequent calcination post-treatments were still needed to remove the extra-framework Ti species as well as the alkali cations before they were used as catalysts. However, the 101 and 102 diffractions overlapped during this post-treatment procedure (Fig. 2.6), indicating the co-existence of another configuration of MWW zeolite, MCM-56 [42, 43]. A structural disorder was believed to occur along the layer stacking direction in MCM-56 zeolite, which possesses larger external surface than normal MWW zeolite. Hence, the Ti-MWW zeolite prepared with linear-type organic molecules showed comparable activity with that synthesized with PI molecules in spite of a poor crystallinity. The small particle sizes and the co-existence of MCM-56 were supposed to compensate the shortage aroused by the poor crystallinity of Ti-MWW prepared with linear SDA molecules.

2.3.2 Synthesis of Ti-MWW by a Dry-Gel Conversion Method

Dry-gel conversion has been proved to be a useful method to prepare several zeolites, such as MFI [44], BEA [45], FER [46], MOR [47], and MTW [48]. Compared with the traditional hydrothermal synthesis method, DGC shows many

Table 2.3 The titanosilicates synthesized at different Si/Ti and K/Si ratios by using various SDAs[a]

Organic SDA	Si/Ti = 40			Si/Ti = 50			Si/Ti = 100		
	$x \leq 0.04$	$x = 0.06$	$x \geq 0.1$	$x = 0.04$	$x = 0.06$	$x = 0.1$	$x = 0.0\ 4$	$x = 0.06$	$x = 0.1$
OCTMAOH	Amor.	MWW + Amor.	MWW + Amor.	MWW	MWW	MFI	MWW	MWW	MFI
HEPMAOH	Amor.	MWW + Amor.	MWW + Amor.	MWW	MWW	MFI	MWW	MWW	MFI
HEXMAOH	MFI	MFI	MFI	MWW	MFI	MFI	MWW	MFI	MFI

Reprinted from Ref. [41], Copyright 2011, with permission from Elsevier

[a] Gel compositions and crystallization conditions, SDA/Si = 0.3; Si/B = 10; H_2O/Si = 30. The crystallization was performed under static conditions at 443 K for 7 days. x represents the K/Si ratio in the gels

Table 2.4 CHN chemical analysis and weight loss of as-synthesized Ti-MWW

Sample	C/N[a]	Weight loss (wt%)[b]		
		<473 K	>473 K	Total
Ti-MWW-HEP	9.7	3.2 (1.1)	15.5 (7.8)	18.7 (8.9)
Ti-MWW-OCT	11.2	2.9 (1.3)	17.6 (10.5)	20.5 (11.8)

Reprinted from Ref. [41], Copyright 2011, with permission from Elsevier
[a] Given by chemical analyses
[b] Given by TGA. The values in parentheses show the amount after acid treatment with 2 M HNO_3

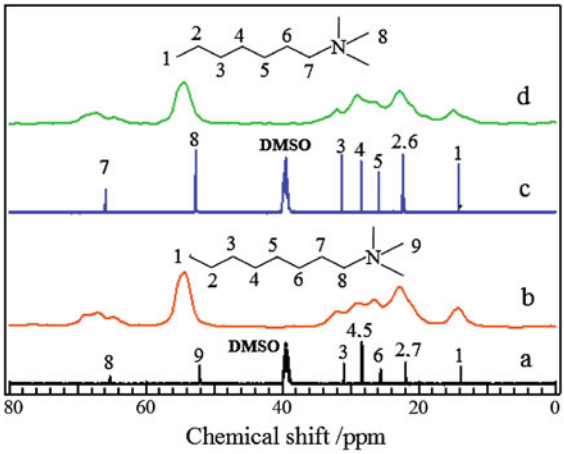

Fig. 2.5 ^{13}C NMR spectra of OCTMAOH (*a*) and HEPMAOH (*c*) in DMSO-d6 solution and ^{13}C CP MAS NMR spectra of Ti-MWW-OCT (*b*) and Ti-MWW-HEP (*d*) both in as-synthesized form. Reprinted from Ref. [41], Copyright 2011, with permission from Elsevier

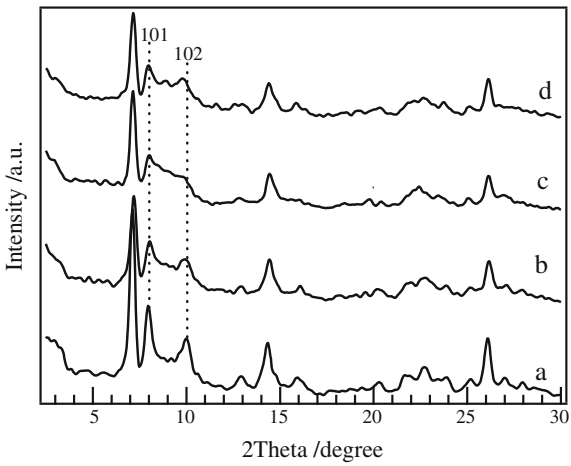

Fig. 2.6 The XRD patterns of acid-treated and calcinced Ti-MWW-OCT (Si/Ti = 50) (*a*), Ti-MWW-OCT (Si/Ti = 100) (*b*), Ti-MWW-HEP (Si/Ti = 50) (*c*), and Ti-MWW-HEP (Si/Ti = 100) (*d*). The as-synthesized samples were treated with 2 M HNO_3 at 373 K for 20 h, and then calcined at 823 K for 10 h. Reprinted from Ref. [41], Copyright 2011, with permission from Elsevier

advantages, including higher yield, shorter crystallization time, and less organic material consumption. Moreover, uniform crystals with much smaller particle sizes were obtained in synthesizing both BEA-type aluminosilicate and titanosilicate with DGC method in comparison with the hydrothermal synthesis [18, 49]. The DGC method further favored the crystallization of BEA-type titanosilicate under Al-free conditions, which was much more difficult in the hydrothermal synthesis method. The DGC method can be divided into two categories in terms of the volatility of organic SDAs, that is, stream assisted crystallization (SAC) and vapor-phase transport (VPT). DGC with volatile SDAs was achieved by the VPT method, in which the SDAs and water were separated from the dried synthetic gels. As for non-volatile SDAs, they were added into the synthetic gels with water placed below them, and then the crystallization was realized with the so-called SAC method.

The DGC method was also applied to synthesis of Ti-MWW zeolite [27] (denoted as Ti-MWW-DGC) and the results are listed in Table 2.5. Both colloidal silica and fumed silica can be used as the Si source. Sodium cations were introduced into the synthetic gels with a Si/Na ratio of 37 when colloidal silica was used as Si source. By using alkali cations-free fumed silica, the crystallization was also achieved, which indicated that the alkali cations were not always necessary. However, too much alkali cations would inhibit the crystallization, yielding amorphous. The B content was decreased greatly with Si/B = 5, compared with Si/B = 0.75 in hydrothermal synthesis. The B atoms are much smaller than Si atoms, which makes it difficult to incorporate the B atoms into the framework. The higher content of boron acid was supposed to be the driving force for the insertion of B atoms into the SiO_2 matrix during the crystallization process. The B content was highly concentrated as no water existed in dry gels, and it was probably the

Table 2.5 The results of Ti-MWW-DGC synthesized by a dry-gel conversion method

No	Silica source	Gel composition			SDA	Time (week)	Product composition		
		Si/Ti	Si/B	Si/Na			Si/Ti	Si/B	Si/Na
1	Colloidal	60	5	37	HMI	2	61	17	114
2	Colloidal	60	3	37	HMI	2	58	13	135
3	Colloidal	60	1	37	HMI	2	54	13	325
4	Colloidal	60	5	37	PI	2	66	16	124
5	Colloidal	60	3	37	PI	2	84	14	–
6	Cab-o-sil	60	5	∞	HMI	2	84	14	∞
7	Colloidal + seed (10 %)	60	12	37	HMI	2	63	18	73
8	Colloidal + seed (10 %)	60	12	37	PI	2	63	18	73
9	Colloidal + seed (10 %)	60	5	37	HMI	1	–	–	–
10	Colloidal + seed (10 %)	60	5	37	PI	1	84	14	454
11	Cab-o-sil + seed (10 %)	60	8	∞	PI	1	58	14	∞
12	Cab-o-sil + seed (10 %)	60	5	∞	HMI	1	–	–	–
13	Cab-o-sil + seed (10 %)	60	5	∞	PI	1	86	14	∞
14	Cab-o-sil + seed (10 %)	30	5	∞	PI	1	28	13	∞
15	Cab-o-sil + seed (50 %)	30	92	∞	PI	1	49	155	∞

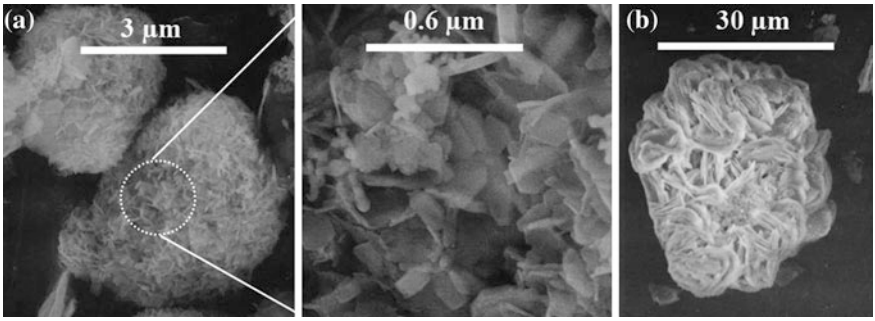

Fig. 2.7 SEM images of Ti-MWW synthesized by hydrothermal method (**a**) and dry-gel conversion method (**b**). Reprinted from Ref. [27], Copyright 2005, with permission from Elsevier

reason why less boron acid was needed in DGC method. The B content was further decreased to Si/B = 12 when 10 wt% of deboronated MWW zeolite was added as seed, meaning that the introduction of seed favored the crystallization process. Moreover, the crystallization process was speeded up upon the addition of seed and Ti-MWW-DGC with a high crystallinity was obtained within 1 week. The Si/B ratio even increased up to 92 when 50 % seed was added into the synthetic gels, the crystallization mechanism of which was not clear. The possibility of post-synthesis via reversible structural conversion occurring on the seed crystals cannot be excluded when such a high content seed was added. This aspect will be described in next section.

Both tetrahedral and octahedral Ti species were formed during the DGC crystallization process. The octahedral Ti species again can be selectively removed with an acid treatment, leaving only a sharp band around 220 nm in the UV–visible spectra. However, the acid treatments lead to the Ti-MWW-DGC zeolite with a higher Si/Ti ratio than hydrothermal synthesized Ti-MWW zeolite, indicating that more Ti species located in the non-framework sites and thus unstable in acid treatment. As mentioned above, uniform crystals with smaller particle sizes were obtained in synthesizing Ti-Beta zeolite with the DGC method. Unfortunately, the particle size of Ti-MWW-DGC was 10–20 times larger than those obtained by hydrothermal synthesis (Fig. 2.7), which certainly imposed significant diffusion problems for both the substrates and the products. Thus, Ti-MWW-DGC showed a much lower activity in the epoxidation of 1-hexene than hydrothermally synthesized Ti-MWW.

2.3.3 Synthesis of Ti-MWW with the Assistant of F^- Ions

The F^- ion is an important accessory ingredient for zeolite crystallization process. With the help of F^- ions, Ti-Beta zeolite can be synthesized under Al-free

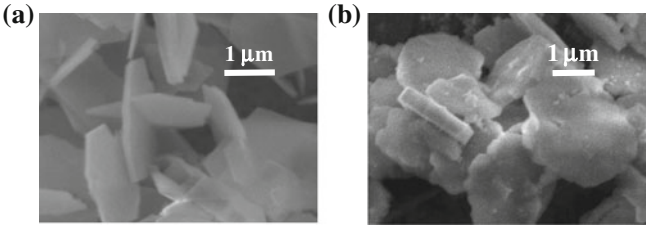

Fig. 2.8 SEM images of Ti-MWW synthesized with the assistant of F^- ions using HMI (**a**) and PI (**b**) as SDA

conditions [50]. In addition, F^- ions can stabilize the double 4-MR units in constructing those zeolites with extra-large pore channels [51–53], especially gemanosilicates. To decrease the amount of B atoms, the F^- ions were also introduced into the synthetic gels of Ti-MWW zeolite. With the help of F^- ions, Ti-MWW zeolite with a high crystallinity (denoted as Ti-MWW-F) can be obtained with the Si/B ratio varying in the range of 1–15. Similar with other zeolites produced from the F^- medium[54], Ti-MWW-F possessed very large particle size and was ten times larger than Ti-MWW-HTS. In conventional hydrothermal synthesis method, Ti-MWW zeolite synthesized with HMI SDA had larger particle size than that synthesized with PI molecules, which was the opposite case in F^- medium. Thus, the Ti-MWW-F-PI particle size was two times larger than that of Ti-MWW-F-HMI (Fig. 2.8). Another special phenomenon was that a band around 330 nm assigned to anatase TiO_2 showed up when PI was used as the SDA molecules in F^- medium. When HMI was used as SDA, only tetrahedral and octahedral coordinated Ti species were involved in the Ti-MWW structure. Since inactive anatase TiO_2 cannot be removed by acid treatment, the HMI molecules were selected as SDA when synthesizing Ti-MWW zeolite in F^- medium.

Some of the Ti-MWW-F lamellar precursor formed 3D MWW structure while some formed an interlayer expanded structure upon the acid treatment which was meant to remove the octahedral coordinated Ti species (Table 2.6). Although the inactive octahedral coordinated Ti species were removed as verified by UV–Vis spectra, the 3D Ti-MWW-F showed very low activity in the epoxidation of cyclohexene. It was supposed that the large particle size of Ti-MWW-F brought about diffusion constrains for the substrates of cyclohexane. However, another interlayer expanded structure obtained upon acid treatment showed largely enhanced activity than the 3D Ti-MWW-F zeolite. This interlayer-expanded Ti-MWW structure has been reported as Ti-YUN-1 [55]. Figure 2.9 shows the TEM images of both 3D Ti-MWW zeolite and interlayer-expanded Ti-MWW zeolite. It can be obviously observed that the layer spacing of interlayer-expanded Ti-MWW zeolite was larger than 3D Ti-MWW zeolite by 2–3 Å. And the structure was supposed to be formed by inserting monomeric Si species into the interlayer space

Table 2.6 Synthesis composition and oxidation of cyclohexene with H_2O_2

Sample No.	Gel				Acid		Cyclohexene	H_2O_2 (%)	
	Si/Ti	Si/B	HMI/Si	HF/Si	Treatment	Phase	Conversion (%)	Conversion	selectivity
1	30	6	1.4	1	50 mL:1 g	Expanded 3D	20.8	28.4	73.2
2	30	6	1.4	0.84	50 mL:1 g	Expanded 3D	13.9	13.9	99.7
3	30	6	1.4	0.6	50 mL:1 g	3D MWW	0.53	0.79	66.9
4	40	6	1	1	30 mL:1 g	3D MWW	2.9	3.3	89.1
5	50	6	1	1	30 mL:1 g	3D MWW	2.1	2.7	77.8
6	60	6	1	1	30 mL:1 g	Expanded 3D	12.3	14.1	87.2
7	70	6	1	1	30 mL:1 g	Expanded 3D	9.5	15.5	62.3
8	80	6	1	1	30 mL:1 g	Expanded 3D	10.5	14.8	70.9
9	100	6	1	1	30 mL:1 g	Expanded 3D	8.3	10.7	77.6

Conditions: cyclohexene, 10 mmol; H_2O_2 (31 wt%), 10 mmol; acetonitrile, 10 mL; cat., 50 mg; temp., 60 °C; time, 2 h

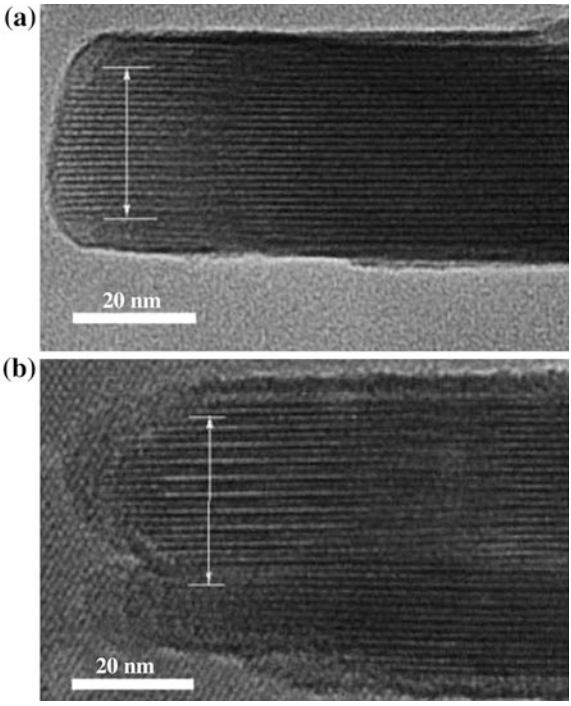

Fig. 2.9 Edge-on TEM image views of 3D Ti-MWW (**a**) and expanded 3D Ti-MWW (**b**). The *arrow* indicates the thickness of 10 MWW layers. Reprinted from Ref. [55], Copyright 2004, with permission from John Wiley and Sons

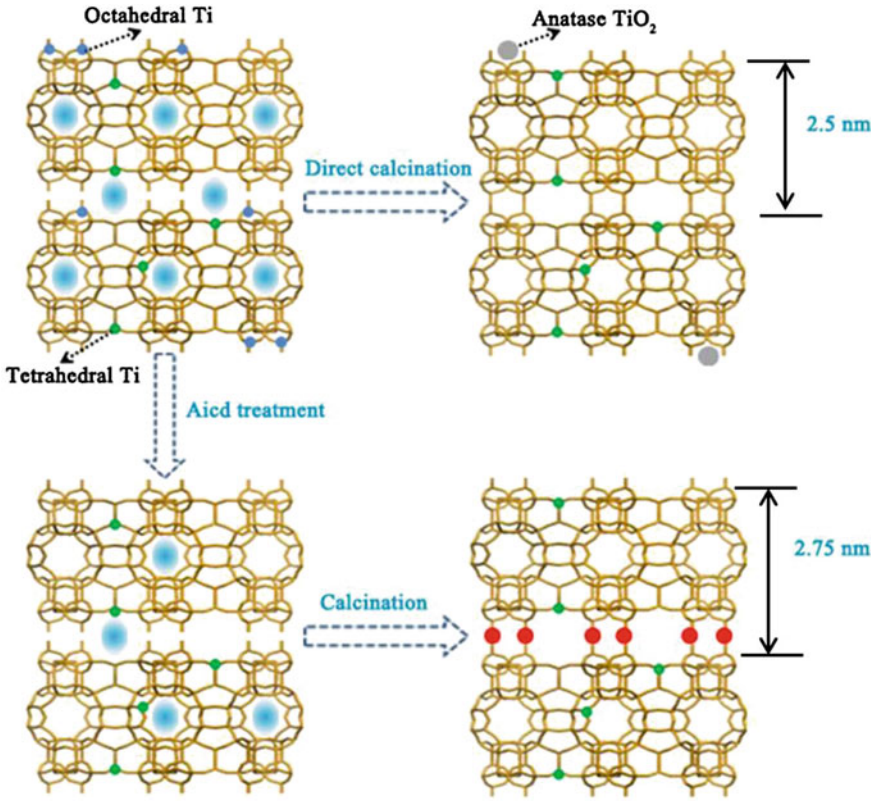

Fig. 2.10 Possible scheme for the formation of expanded Ti-MWW structure

upon acid treatment (Fig. 2.10), which will be described in detail in Sect. 3.5. With larger interlayer space, the diffusion constrain was largely released and the substrate of cyclohexene can easily reach the active Ti sites. Thus, Ti-MWW-F zeolites with interlayer expanded structure showed extremely high activities.

2.4 Boron-Free Ti-MWW Synthesis

2.4.1 Synthesis of Ti-MWW with Dual Structure-Directing Agents

Organic SDAs play two different roles in synthesizing MWW lamellar precursor, including filling the intralayer 10-MR channels and stabilizing interlayer spaces. ITQ-1 [56], pure silica MWW zeolite, was prepared with dual SDAs, HMI and TMAadOH. TMAadOH with larger molecular size locate in the interlayer spaces

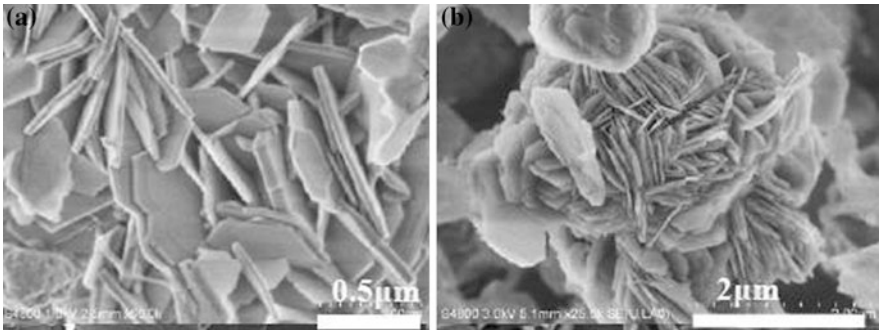

Fig. 2.11 SEM images of Ti-MWW using dual structure-directing agents with Si/Ti ratio of 50 (**a**) and 100 (**b**)

Table 2.7 Chemical composition of Ti-MWW synthesized with hydrothermal method

SDAs	%N	%C	%H	C/N	TG[a]
HMI[b]	3.03	16.45	3.41	5.82	24.6
TMAdaOH + HMI	1.81	13.30	2.77	11.49	21.1
TMAdaOH + HMI[c]	1.20	7.82	2.07	7.60	13.8
TMAdaOH[b]	1.01	10.53	1.92	12.16	16.7

[a] Weight loss by thermogravimetric analysis to 1073 K
[b] Synthesized with Si/B = 0.75
[c] Acid treatment with 2 M HNO_3

while smaller HMI molecules diffuse into the intralayer 10-MR channels. The structure of ITQ-1 zeolite was constructed by the corporation of these two organic molecules in the synthetic gels. Stimulated by this crystallization process, Liu et al. synthesized Ti-MWW zeolite (denoted as Ti-MWW-Dual) under B-free conditions by hydrothermal synthesis method with the help of the above two organic molecules and K^+ ions [57]. In the conventional hydrothermal method, a large amount of boron acid (Si/B = 0.75) was needed with either HMI or PI as SDA. Nevertheless, the B content can be decreased to zero in the dual SDAs system. On the other hand, the amount of organic SDA was decreased a lot, too. When PI or HMI was used to direct the construction of MWW structure, the ratio of PI/Si or HMI/Si was about 1.4, while the ratio in the final product was only 0.1. That is, most of the organic molecules were wasted during the crystallization process. The total amount of organic molecules in the dual structure-directing system was enough at the (HMI + TMAadOH)/Si ratio of 0.56, which was less than half of that used in the system with single SDA. Ti-MWW zeolite with a high crystallinity can be obtained when the ratio of TMAadOH/HMI ranged from 0.2 to 1.2. The product with the C/N ratio of 11.49 (Table 2.7), a value between the C/N ratio of TMAadOH molecule and HMI molecule, contained about 20 % HMI molecules and 80 % TMAadOH molecules. After an acid treatment, the C/N ratio was

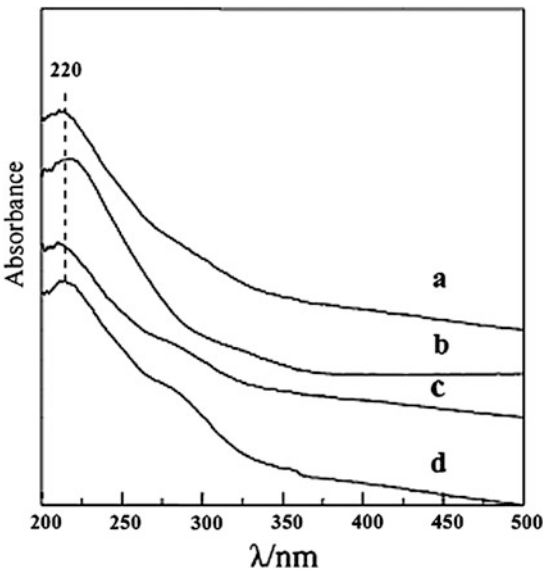

Fig. 2.12 UV–visible spectra of as-made Ti-MWW synthesized using dual structure-directing agents with the Si/Ti ratio of (*a*) 100, (*b*) 50, (*c*) 30 and (*d*) 20

decreased to 7.60, more close to the C/N ratio of HMI molecules, meaning that most of the TMAadOH molecules were removed during the acid treatment and the remaining HMI molecules were hardly washed out of the structure. Hence, it can be inferred that HMI molecules was stuck in the intralayer 10-MR channels while the TMAadOH molecules located in the interlayer spaces, which was similar with that in synthesizing ITQ-1 zeolite.

Although the alkali cations in the synthetic gels of titanosilicates would retard the insertion of Ti atoms into the framework, minute alkali cations was necessary in the crystallization process in some special cases, such as the synthesis of Ti-MWW-Dual zeolite. When the ratio of K^+/Si was lower than 0.05, only amorphous was obtained. The appropriate ratio of K^+/Si was set at 0.07 after detailed investigation. Too much K^+ cations would cause the formation of other lamellar structures other than MWW zeolite. The K^+ cations would be removed by an acid treatment before Ti-MWW zeolite was used as the catalyst in epoxidation reactions.

As shown in the SEM images (Fig. 2.11), these crystals of Ti-MWW-Dual zeolite possessed uniform particle size of 0.5 × 0.5 × 0.1 μm, which was similar with that of Ti-MWW crystals synthesized with the help of PI by hydrothermal method. The change of Ti content hardly affects the aggregation and the particle sizes. A synthetic gel with the Si/Ti ratio of 20 can still yield pure Ti-MWW zeolite, the crystallinity of which was very high, though. Only very weak band was observed around 260 nm in the UV–visible spectra (Fig. 2.12) meaning that Ti-MWW-Dou zeolite has much less octahedral Ti species than those synthesized with other methods. That is probably because Ti species can be inserted into the framework more easily without the competition of B atoms in the synthesis gels.

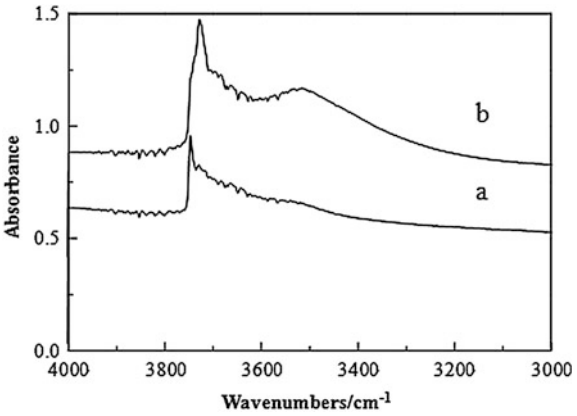

Fig. 2.13 FTIR spectra of Ti-MWW synthesized using dual structure-directing agents (*a*) and PI (*b*) with Si/Ti = 50 in hydroxyl stretching region

The existence of framework Ti species induced a band around 960 cm^{-1} in the IR spectra measured under air condition. The band shifted to 930 cm^{-1} when the sample was pretreated in vacuum. This was supposed to be related to the absence of B atoms, because a shoulder band would also appear besides the original band at 960 cm^{-1} in the IR spectra of Ti-MWW zeolite synthesized with B atoms pretreated in vacuum. However, the real reason is not clear. In the hydroxyl stretching vibration regions, Ti-MWW-Dou zeolite synthesized in the absence of B atoms showed a band round 3750 cm^{-1} with lower intensity than that synthesized with the help of B atoms (Fig. 2.13). The band around 3750 cm^{-1} appearing in the IR spectra of Ti-MWW samples after evacuation was attributed to the terminal Si–OH groups. B atoms with small cation radii were loosely incorporated into the framework of Ti-MWW zeolite probably inducing much more defects and more Si–OH groups. Hence, the Ti-MWW zeolite synthesized in the presence of B atoms was more hydrophilic, which was caused by the existence of numerous terminal hydroxyl groups.

With the presence of K^+ cations, Ti-MWW zeolite was almost inactive in the epoxidation reactions. After an acid treatment, the K^+ cations would be almost completely removed and Ti-MWW-Dual showed good performance as the catalysts in the epoxidation reactions, which means the existence of K^+ cations indeed poisoned the Ti active sites. In the epoxidation of 1-hexene, the Ti-MWW-Dou zeolite showed higher activity than that synthesized with sole organic agent, although the particle sizes of the former was a little bit larger. The absence of B atoms favored the insertion of Ti atoms, decreased the amount of defects and enhanced the hydrophobicity, which is the reason why Ti-MWW-Dual synthesized with the coexistence of HMI and TMAadOH molecules was more active. Ti-MWW-Dual zeolite was also stable enough to resist the leaching of Ti species during liquid phase reactions, the activity of which was remained even after fifth catalytic runs.

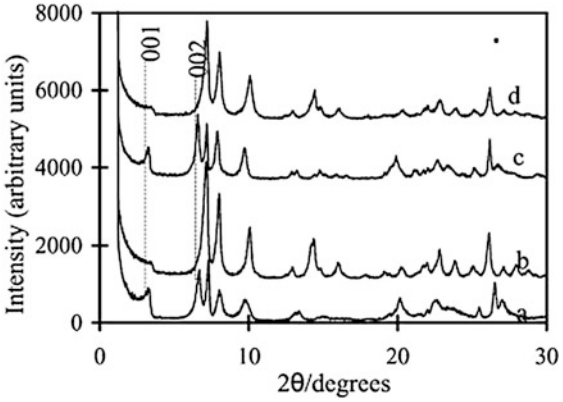

Fig. 2.14 X-Ray diffraction patterns of as-synthesized B-MWW (Si/B = 11) (*a*), deboronated MWW (Si/B > 1000) (*b*), Ti-MWW (Si/Ti = 30) precursor (*c*), and sample *c* treated with 2 M HNO_3 and calcined (*d*). Reprinted from Ref. [28], Copyright 2002, with permission from Royal Society of Chemistry

2.4.2 Synthesis of B-Free Ti-MWW Through Reversible Structure Conversion

The lamellar zeolite can be converted to a rigid 3D zeolite upon calcination, during which condensation between silanols on the up and down layers would take place. And the reversibility of this process was supposed to hardly happen because of the strong Si–O–Si bonds connecting the layers. However, several cases involving the change from 3D zeolite to 2D layered zeolite have been found recently. Germanosilicate UTL zeolite with double 4-MR structures rich in Ge atoms easily hydrolyzes to lamellar zeolite with layers similar to FER layers in mild acid conditions, which is also believed to be a promising way to expand the family of layered zeolites [58, 59]. Another example is the reversibility between the 3D MWW structure and its lamellar precursor. That is, 3D MWW structure can be changed to MWW lamellar precursor with the help of amine molecules [28].

The reversibility can be applied to preparing MWW titanosilicate in the absence of B atoms using a post-synthesis method (denoted as Ti-MWW-PS) [28]. This method involves the preparation of high silica MWW zeolite and the incorporation of Ti atoms during the structural conversion process. The structural changes can be revealed by the XRD patterns as shown in Fig. 2.14. The 001 and 002 diffraction peaks disappeared after calcination and deboronation procedures which indicated that a rigid 3D MWW structure was formed. When the deboronated MWW zeolite (Si/B > 1000) was subjected to the structural conversion process in the presence of Ti source (TBOT), the 001 and 002 diffraction peaks were restored, meaning the lamellar structure was again obtained. Several organic amines including HMI, PI, pyridine, and piperazine were employed to direct this conversion process. However, the reversible structural conversion only occurred in the presence of HMI and

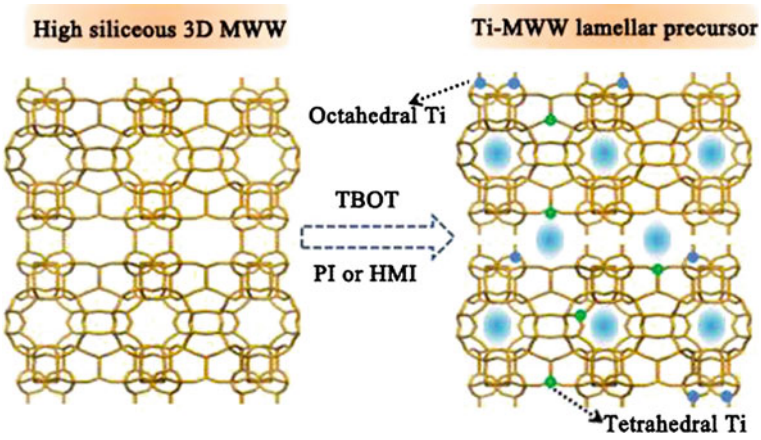

Fig. 2.15 Graphic description for the postsynthesis of boron-free Ti-MWW via reversible structure conversion

PI molecules, which were two typical structure-directing agents for preparing MWW zeolite. Reorganization seemed to have happened between the MWW structure and the structural-directing agents in the conversion process. The highly siliceous MWW zeolite (Si/B > 1000) was prepared through severe acid treatment of the calcined MWW borosilicate, creating numerous vacancies in the framework. The alkalinity provided by the amine molecules in the conversion process would cleave the Si–O–Si bonds between layers, making the interlayer space larger to favor the diffusion of Ti precursors into the vacancies (Fig. 2.15). All the Ti atoms in the synthetic gels can be inserted into the framework, indicating that the

Table 2.8 1-Hexene oxidation over various titanosilicates with acetonitrile as a solvent[a]

Cat	Si/Ti	1-Hexene		H_2O_2	
		Conversion %	TON	Conversion %	Efficiency %
Ti-MWW-OCTMAOH	95	16.5	176	19.2	86
	132	14.6	215	17.3	84
Ti-MWW-Dual	35	42.6	180	52.5	81
	103	42.2	488	51.2	82
Ti-MWW-HMI	46	37.5	213	40.3	93
	72	22.4	198	25.6	88
Ti-MWW-PS	58	60.7	480	67.9	93
	100	49.8	500	50.1	92
Ti-MWW-DGC	58	1.7	42	7	33
	84	2.4	69	19	16
Ti-MWW-F	70	51.1	465	58	88.1
	356[b]	16.3	706	19.7	82.7

[a] Reaction conditions: bath reactor; cat., 50 mg; substrate, 10 mmol; H_2O_2, 10 mmol; MeCN 10 mL; temp., 333 K; time, 2 h

[b] Ti-MWW with expanded structure

post-synthesis method was effective for Ti incorporation. Both tetrahedral and octahedral Ti species were found in the Ti-MWW zeolite prepared by structure conversion method, which was the same as hydrothermal synthesized Ti-MWW zeolite. The extra-framework Ti species was selectively removed by an acid treatment, resulting in a highly active catalyst. The B-free Ti-MWW-PS zeolite showed improved catalytic activity compared with the B-containing and B-less Ti-MWW zeolite, i.e., TON and epoxide selectivity in the epoxidation of both bulky cyclohexene and linear alkyl alcohol, which was assumed to be due to the decrease of B-related acidity and framework electronegativity (Table 2.8).

References

1. Bellussi G, Rigutto MS (2001) Metal ions associated to molecular sieve frameworks as catalytic sites for selective oxidation reactions. Stud Surf Sci Catal 137:911–955
2. Ratnasamy P, Srinivas D, Knözinger H (2004) Acitve sites and reactive intermediates in titanium silicate molecular sieves. Adv Catal 48:1–169
3. Wu P, Komatsu T, Yashima T (1996) Characterization of titanium species incorporated into dealuminated mordenites by means of IR spectroscopy and ^{18}O-exchange technique. J Phys Chem 100:10316–10322
4. Corma A, Camblor MA, Esteve PA et al (1994) Activity of Ti-Beta catalyst for selective oxidation of alkenes and alkanes. J Catal 145:151–158
5. Tuel A (1995) Synthesis, characterization, and catalytic properties of the new TiZSM-12 zeolite. Zeolites 15:236–242
6. Wu P, Komatsu T, Yashima T (1997) Ammoximation of Ketones over titammium mordenite. J Catal 168:400–411
7. Wu P, Komatsu T, Yashima T (1998) Hydroxylation of aromatics with hydrogen peroxide over titanosilicates with MOR and MFI structures: effect of Ti peroxo species on the diffusion and hydroxylation activity. J Phys Chem B 102:9297–9303
8. Xu H, Zhang YT, Wu HH et al (2011) Postsynthesis of mesoporous MOR-type titanosilicate and its unique catalytic properties in liquid-phase oxidations. J Catal 25:263–272
9. van der Waal JC, Rigutto MS, van Bekkum H (1998) Zeolite titanium beta as a selective catalyst in the epoxidation of bulky alkenes. Appl Catal A: General 167:331–342
10. Blasco T, Corma A, Navarro MT et al (1995) Synthesis, characterization, and catalytic activity of Ti-MCM-41 structures. J Catal 156:65–74
11. Leonowicz ME, Lawton JA, Lawton SL et al (1994) MCM-22: a molecular sieve with two independent multidimensional channel systems. Science 264:1910–1913
12. Corma A, Martínez-Soria V, Schnoeveld E (2000) Alkylation of benzene with short-chain olefins over MCM-22 zeolite: catalytic behavior and kinetic mechanism. J Catal 192:163–173
13. Corma A, Corell C, Pérez-Pariente J (1995) Synthesis and characterization of MCM-22 zeolite. Zeolites 15:2–8
14. Komura K, Murase T, Sugi Y et al (2010) Synthesis of boron-containing CDS-1 zeolite by topotactic dehydration condensation of [B]-PLS-1 prepared from layered silicate H-LDS. Chem Lett 39:948–949
15. Wu P, Liu H, Komatsu T et al (1997) Synthesis of ferrisilicate with the MCM-22 structure. Chem Commun 7:663–664
16. Ahedi RK, Kotasthane AN (1998) Synthesis of FER titanosilicates from a non-aqueous alkali-free seeded system. J Mater Chem 8:1685–1686

17. Kubota Y, Koyama Y, Yamada T et al (2008) Synthesis and catalytic performance of Ti-MCM-68 for effective oxidation reactions. Chem Commun 46:6224–6226
18. Tatsumi T, Jappar N (1998) Properties of Ti-Beta zeolites synthesized by dry-gel conversion and hydrothermal methods. J Phys Chem B 102:7126–7131
19. Lv AL, Xu H, Wu HH et al (2011) Hydrothermal synthesis of high-silica mordenite by dual-templating method. Micropor Mesopor Mater 145:80–86
20. Maschmeyer T, Ray F, Sankar G et al (1995) Heterogeneous catalysts obtained by grafting metallocene complexes onto mesoporous silica. Nature 378:159–162
21. Morey MS, O'Brien S, Schwarz S et al (2000) Hydrothermal and postsynthesis surface modification of cubic, MCM-48, and ultralarge pore SBA-15 mesoporous silica with titanium. Chem Mater 12:898–911
22. Jappar N, Xia Q, Tatsumi T (1998) Oxidation activity of Ti-Beta synthesis by a dry-gel conversion method. J Catal 180:132–141
23. Corma A, Díaz U, Fornés V et al (1999) Ti/ITQ-2, a new material highly active and selective for the epoxidation of olefins with organic hydroperoxides. Chem Commun 9:779–780
24. Levin D, Chang CD, Luo S et al (2000) US 6 114 551
25. Millini R, Perego G, Parker WO Jr et al (1995) Layered structure of ERB-1 microporous borosilicate precursor and its intercalation properties towards polar molecules. Micropor Mater 4:221–230
26. Wu P, Tatsumi T, Komatsu T et al (2001) A novel titanosilicate with MWW Structure. I. Hydrothermal synthesis, elimination of extraframework titanium, and characterizations. J Phys Chem B 105:2897–2905
27. Wu P, Miyaji T, Liu YM et al (2005) Synthesis of Ti-MWW by a dry-gel conversion method. Catal Today 99:233–240
28. Wu P, Tatsumi T (2002) Preparation of B-free Ti-MWW through reversible structural conversion. Chem Commun 10:1026–1027
29. Jorda E, Tuel A, Teissier R et al (1997) TiF4: An original and very interesting precursor to the synthesis of titanium containing silicalite-1. Zeolites 19:238–245
30. Balducci L, Bianchi D, Bortolo R et al (2003) Direct oxidation of benzene to phenol with hydrogen peroxide over a modified titanium silicalite. Angew Chem Int Ed 42:4937–4940
31. Wang X, Guo X (1999) Synthesis, characterization and catalytic properties of low cost titanium silicalite. Catal Today 51:177–186
32. Wu P, Tatsumi T, Komatsu T et al (2001) A novel titanosilicate with MWW structure: II. Catalytic properties in the selective oxidation of alkenes. J Catal 202:245–255
33. Zones SI, Santilli D (1992) In: Von Ballmoos R, Higgins JB, Treacy MMJ (eds) Proceedings of the 9th international zeolite conference, Montreal. Butterworth-Heinemann, Stoneham, p 171
34. Wagner P, Nakagawa Y, Lee GS et al (2000) Guest/host relationships in the synthesis of the novel cage-based zeolites SSZ-35, SSZ-36, and SSZ-39. J Am Chem Soc 122:263–273
35. Puppe L (1984) U.S. Pat., 4439409
36. Zones SI, Hwang S-J, Davis ME (2001) Studies of the synthesis of SSZ-25 zeolite in a "Mixed-Template" system. Chem Eur J 7:1990–2001
37. Zones SI (1989) U.S. Pat., 4826667
38. Lee S-H, Shin C-H, Hong SB (2003) Synthesis of zeolite MCM-22 using N,N,N,N′,N′,N′,-Hexamethyl-1,5-pentanediaminium and alkali metal cations as structure-directing agents. Chem Lett 32:542–543
39. Hong SB, Min H-K, Shin C-H et al (2007) Synthesis, crystal Structure, characterization, and catalytic properties of TNU-9. J Am Chem Soc 35:10870–10885
40. Liu N, Liu YM, Yue CC et al (2007) A new synthesis route for MWW analogues using octyltrimethylammonium cations as structure-directing agents under alkali-free conditions. Chem Lett 36:916–917
41. Yue CC, Xie W, Liu YM et al (2011) Hydrothermal synthesis of MWW-type analogues using linear-type quaternary alkylammonium hydroxides as structure-directing agents. Micropor Mesopor Mater 142:347–353

42. Fung AS, Lawton SL, Roth WJ (1994) U.S. Pat., 5362697
43. Corma A, Diaz U, Fornés V et al (2000) Characterization and catalytic activity of MCM-22 and MCM-56 compared with ITQ-2. J Catal 191:218–224
44. Bandyopadhyay R, Kubota Y, Sugimoto N et al (1999) Synthesis of borosilicate zeolites by the dry gel conversion method and their characterization. Micropor Mesopor Mater 32:81–91
45. Hari Prasad Rao PR, Matsukata M (1996) Dry-gel conversion technique for synthesis of zeolite BEA. Chem Commun 12:1441–1442
46. Matsukata M, Nishiyama N, Ueyama K et al (1996) Crystallization of FER and MFI zeolites by a vapor-phase transport method. Micropor Mater 7:109–117
47. Wang J, Cheng X, Guo J et al (2006) High-silica MOR type zeolite self-transformed from dry aluminosilicate gel in OSAs-free and fluoride-free reactant system. Micropor Mesopor Mater 96:307–313
48. Matsukata M, Ogura M, Osaki T et al (1999) Conversion of dry gel to microporous crystals in gas phase. Topics Catal 9:77–92
49. Hari Prasad Rao PR, Leon y Leon CA, Ueyama K et al (1998) Synthesis of BEA by dry gel conversion and its characterization. Micropor Mesopor Mater 21:305–313
50. Blasco T, Camblor MA, Corma A et al (1996) Unseeded synthesis of Al-free Ti-β zeolite in fluoride medium: a hydrophobic selective oxidation catalyst. Chem Commun 20:2367–2368
51. Blasco T, Corma A, Díaz-Cabanas MJ et al (2004) Synthesis, characterization, and framework heteroatom localization in ITQ-21. J Am Chem Soc 126:13414–13423
52. Jiang J, Jorda JL, Yu J et al (2011) Synthesis and structure determination of the hierarchical meso-microporous zeolite ITQ-43. Science 333:1131–1133
53. Hernández-Rodríguez M, Jordá JL, Rey F et al (2012) Synthesis and structure determination of a new microporous zeolite with large cavities connected by small pores. J Am Chem Soc 134:13232–13235
54. Schreyeck L, Caullet P, Mougenel J-C et al (1995) A layered microporous aluminosilicate precursor of FER-type zeolite. J Chem Soc Chem Commun 21:2187–2188
55. Fan WB, Wu P, Namba S et al (2004) A titanosilicate that is structurally analogous to an MWW-type lamellar precursor. Angew Chem 117:6877–6881
56. Camblor MA, Corell C, Corma A et al (1996) A new microporous polymorph of silica isomorphous to zeolite MCM-22. Chem Mater 8:2415–2417
57. Liu N, Liu YM, Xie W et al (2007) Hydrothermal synthesis of boron-free Ti-MWW with dual structure-directing agents. Stud Surf Sci Catal 170:464–469
58. Roth WJ, Shvets OV, Shamzhy M et al (2011) Postsynthesis transformation of three-dimensional framework into a lamellar zeolite with modifiable architecture. J Am Chem Soc 133:6130–6133
59. Verheyen E, Joos L, Van Havenbergh K et al (2012) Design of zeolite by inverse sigma transformation. Nat Mater 11:1059–1064

http://www.springer.com/978-3-642-39114-9

MWW-Type Titanosilicate
Synthesis, Structural Modification and Catalytic Applications to Green Oxidations

Wu, P.; Xu, H.; Xu, L.; Liu, Y.; He, M.

2013, VIII, 125 p. 79 illus., 25 illus. in color., Softcover
ISBN: 978-3-642-39114-9